Available online at www.sciencedirect.com
SCIENCE DIRECT
Surface Science 600 (2006) 468–477
SURFACE SCIENCE
www.elsevier.com/locate/susc

Formation of vinylidene and vinylene by selective reactivity of Si(1 0 0)2 × 1 towards *iso*, *cis* and *trans* isomers of dichloroethylene

X.J. Zhou, Z.H. He, K.T. Leung *

Department of Chemistry, University of Waterloo, Waterloo, Ont., Canada N2L 3G1

Received 12 July 2005; accepted for publication 24 October 2005
Available online 7 December 2005

Abstract

The room temperature (RT) chemisorption of three (*iso*, *cis* and *trans*) isomers of dichloroethylene (DCE) on Si(1 0 0)2 × 1 have been investigated by X-ray photoelectron spectroscopy (XPS) and temperature programmed desorption (TPD). Unlike ethylene, the lack of molecular desorption features in the TPD data effectively rules out the cycloaddition adsorption mechanism for all three isomers. XPS spectra show that *cis*- and *trans*-DCE adsorb dissociatively on the 2 × 1 surface in equal proportion as mono-σ bonded 2-chlorovinyl and di-σ bonded vinylene adspecies, which could be produced by dechlorination mechanisms involving the proposed tri-atom π-complex and diradical intermediates, respectively. Acetylene (*m*/*z* 26) evolution from 2-chlorovinyl adspecies at 590 K and vinylene at 750 K are also observed for both *cis*- and *trans*-DCE, further confirming the common adsorption mechanisms for these geometrical isomers and the relative stabilities of the adspecies. In contrast, only vinylidene adspecies is found for *iso*-DCE, which indicates that the high ionicity of the $=CCl_2$ group favours the diradical dechlorination mechanism. The single *m*/*z* 26 desorption peak for *iso*-DCE adspecies observed at a higher temperature (780 K) than *cis* and *trans* isomers is consistent with the higher adsorption energy of vinylidene than vinylene on Si(1 0 0) obtained in our ab initio calculations. The different relative locations of the Cl atoms in these isomers therefore play a crucial role in controlling the adsorption and thermal evolution on Si(1 0 0)2 × 1. The selective reactivity of the 2 × 1 surface towards these isomers can be used to generate vinylene or vinylidene templates from their corresponding adspecies.

Keywords: Dichloroethylene; *iso*, *cis* and *trans* isomers; X-ray photoelectron spectroscopy; Temperature programmed desorption; Chemisorption; Isomer effects

1. Introduction

In comparison to the Si(1 1 1)7 × 7 surface, the Si(1 0 0)2 × 1 surface provides relatively simple surface structure with well-defined dimer rows that exhibit rich chemical properties analogous to disilenes. The 2 × 1 surface continues to provide one of the most important platforms for developing both fundamental understanding of organosilicon chemistry and emerging applications in organic functionalization of silicon surfaces, molecular scale electronics, templates for building nanoscale devices, etc. [1–6]. Modification of the Si surfaces by a variety of organic molecules, particularly their surface interactions and reaction mechanisms, has been extensively investigated by a wide range of surface analytical techniques, including electron energy loss spectroscopy (EELS) [7–9], Fourier transform infrared spectroscopy (FTIR) [4], Auger electron spectroscopy (AES) [10–13], X-ray photoelectron spectroscopy (XPS) [14,15], scanning tunnelling microscopy (STM) [15,16], near-edge X-ray absorption fine structure (NEXAFS) [5], and temperature programmed desorption (TPD) [12–14,17]. These experimental studies have also been complemented by various ab initio quantum mechanical calculations [18–21].

Although it has been generally accepted that alkenes and alkynes react with Si(1 0 0)2 × 1 via a cycloaddition reaction pathway, the nature and reaction mechanism of

* Corresponding author.
E-mail address: tong@uwaterloo.ca (K.T. Leung).

0039-6028/$ - see front matter © 2005 Elsevier B.V. All rights reserved.
doi:10.1016/j.susc.2005.10.050

the initial adsorption is still under intense debate [22]. In particular, two possible intermediate states, involving π electron interactions in the form of a tri-atom π-complex (Structure I) or mono-σ bonding interactions in the form of a diradical (Structure II) [23–25] with a substrate atom, have been proposed for the cycloaddition mechanism [22].

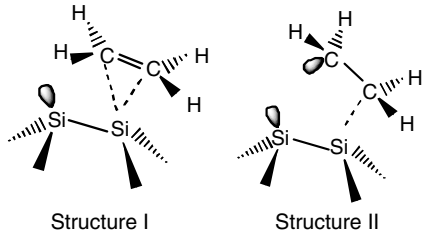

Structure I Structure II

According to ab initio calculations [25], both intermediates are found to be kinetically feasible, with the diradical intermediate generally more favourable than the tri-atom π-complex. To date, only the tri-atom π-complex has been recently observed as a plausible precursor state at 58–90 K for vinyl bromide on Si(1 0 0)c(4 × 2), which has a similar local structure as the 2 × 1 surface, by Nagao et al. using high resolution EELS [8]. This precursor state is believed to lead to the formation of the di-σ bonded bromoethane-1,2-diyl adspecies at 58–90 K similar to that of ethylene adsorption on Si(1 0 0)2 × 1. Nagao et al. also reported the presence of dissociated Br atoms [8], which indicates that dehalogenation is also an important reaction pathway for halogenated alkenes. Furthermore, for vinyl bromide and vinyl iodide initially adsorbed via π-interaction with a metal surface such as Cu(1 0 0) at 100 K, Yang et al. observed the reconstitution of the C=C bond upon annealing to 160 K [26]. Unlike the earlier studies at low temperature, our recent XPS and TPD study shows that dibromoethylene (DBE) primarily undergoes dissociative adsorption on Si(1 0 0)2 × 1 by single or double dehalogenation at room temperature (RT) [14]. In contrast to the commonly proposed cycloaddition adsorption mechanism involving C rehybridization from sp^2 to sp^3, we proposed a different mechanism (insertion mechanism) to account for the observed dissociative adsorption. In this mechanism, the Si atom is effectively inserted into a C–Br bond (with the formation of the Si–C and Si–Br bonds) by breaking the C–Br and Si–Si bonds, while the C=C bond remains intact. The observed dissociative adsorption is consistent with the stronger bond strength of Si–Br (82 kcal/mol) than that of C–Br (67 kcal/mol) [27].

The molecular structure of the organic adsorbate plays a pivotal role in the adsorption mechanism and the reaction selectivity of the resulting adstructures. For example, different functional groups such as the vinyl and phenyl groups in styrene have been found to affect the reactivity on Si(1 0 0)2 × 1 differently [4]. Geometrical isomers such as *cis*- and *trans*-2-butene could also exert different steric conformational effects on Si(1 0 0)2 × 1 [28]. The different thermal stabilities of these isomers as inferred by Kiskinova and Yates from their TPD experiments could be due to the different adsorption geometries imposed by their corresponding molecular conformational specificities [28], which is in good accord with the adsorption stereoselectivity of individual butene molecules observed by Lopinski et al. in a STM study [29]. Similar observations have also been made for the adsorption of *cis*- and *trans*-dichloroethylene (DCE) on Pt(1 1 1) [30] and of *cis*- and *trans*-dideuterated ethylene on Si(1 0 0)2 × 1 [24]. Very recently, our group has investigated the thermal surface chemistries of a series of DCE adsorbates, including the *cis* and *trans* geometrical isomers of 1,2-DCE and their structural isomeric homolog, 1,1- or *iso*-DCE, on Si(1 1 1)7 × 7 by using vibrational EELS and TPD [31]. In particular, both *cis*- and *trans*-DCE are found to exhibit similar RT adsorption properties on the 7 × 7 surface, in contrast to the notable differences observed for *iso*-DCE [31]. These experiments reveal the formation of novel adstructures including vinylene, vinylidene and their chlorinated derivatives, and rule out the cycloaddition mechanism. Dehalogenation has also been identified as a primary process common to all three isomers, in good accord with that observed for perchloroethylene on Si(1 0 0)2 × 1 [32].

In the present work, we compare the RT adsorption and thermal evolution properties of the three isomers (*iso*, *cis* and *trans*) of DCE on Si(1 0 0)2 × 1 and with those found on Si(1 1 1)7 × 7 [31] and metal surfaces [30]. These three isomers are fundamentally interesting because of their differences in molecular structure and local charge distribution, which could produce important effects on the surface chemistry. Using ab initio density functional calculations, we have estimated the APT (atomic polar tensor) atomic charge at the C sites. The respective atomic charges for the C atom of the ($=C^{Cl}_{H}$) component for *cis*-DCE (+0.20 a.u.) and *trans*-DCE (+0.25 a.u.) are found to be similar. In contrast, the APT charge at the C atom of the ($=C^{Cl}_{Cl}$) component (+0.76 a.u.) is considerably more electropositive than that of the ($=C^{H}_{H}$) component (−0.30 a.u.). The strong electrophilic (and dipolar) property of *iso*-DCE is therefore expected to play an important role in controlling the surface chemistry.

2. Experimental details

The experimental setup and procedure have been described in detail elsewhere [12]. Briefly, all the experiments were performed in a home-built dual-chamber ultra-high vacuum (UHV) system with a base pressure better than 1×10^{-10} Torr. Sample preparation was performed in the upper chamber equipped with an ion-sputtering gun for sample cleaning, and a four-grid retarding-field optics for both reverse-view low energy electron diffraction (LEED) and Auger electron spectroscopy. A 14 × 7 mm^2 substrate was cut from a single-side polished p-type B-doped Si(1 0 0) wafer (0.4 mm thick) with a resistivity of 0.0080–0.0095 Ω cm. Details of the sample mounting and prepara-

tion procedures have also been given in our earlier work [12]. The liquid chemicals, *iso*-DCE (99% purity), *cis*-DCE (97% purity) and *trans*-DCE (98% purity), were purchased from Aldrich and thoroughly degassed by repeated freeze–pump–thaw cycles prior to use. Exposure of individual chemical to the Si sample was achieved by backfilling the preparation chamber to an appropriate pressure (as monitored by an uncalibrated ionization gauge) with a variable precision leak valve. All exposures (in units of Langmuir, $1\ \mathrm{L} = 1 \times 10^{-6}$ Torr s) were performed at RT and a saturation coverage was used for all the TPD and XPS experiments unless stated otherwise.

Both the TPD and XPS experiments were conducted in the lower analysis chamber. For the TPD experiments, a differentially pumped 1–300 amu quadrupole mass spectrometer was used to monitor the desorbates, along with a home-built programmable proportional–integral–differential temperature controller used to provide linear temperature ramping at an adjustable heating rate, typically set at 2 K/s [12]. The absolute accuracy of our temperature measurement obtained by an uncalibrated type K thermocouple directly attached to the sample was estimated to be ±20 K. XPS experiments were performed by using an electron spectrometer consisting of a hemispherical analyser (of 100 mm mean radius) and a triple-channeltron detector, with a twin-anode X-ray source that provided unmonochromatic AlKα radiation (with a photon energy 1486.6 eV). XPS spectra were collected with an acceptance angle of ±4° at normal emission from the silicon sample, and with a constant pass energy of 50 eV giving an effective energy resolution of 1.4 eV full-width-at-half-maximum (for the Si 2p photopeak). The binding energy scale of the XPS spectra presented in the present work has been calibrated to the Si 2p feature of the bulk at 99.3 eV [33]. Spectral fitting and deconvolution based on residual minimization with Gaussian–Lorentzian lineshapes were performed by using the CasaXPS software. For temperature-dependent XPS measurements, the sample was flash-annealed to the preselected temperature and quenched to RT before collecting the XPS spectra. In order to avoid ambiguity in the quantification of the surface Cl content based on the Cl 2p photopeak at 200 eV (due to the often ill-defined background contribution arising from the nearby Si 2s feature at 151 eV), the Cl 2s photopeak at 270 eV was used instead in all the experiments.

3. Results and discussion

3.1. Room-temperature chemisorption

Fig. 1 compares the Cl 2s and C 1s XPS spectra of 50 L *iso*-, *cis*- and *trans*-DCE exposed to Si(100)2 × 1 at RT. For all three isomers, the Cl 2s features for the Si–Cl and C–Cl components cannot be resolved with our present XPS apparatus and both contribute to the strong photopeak at 270.3 eV. This assignment is consistent with the small energy difference found for the corresponding orbital

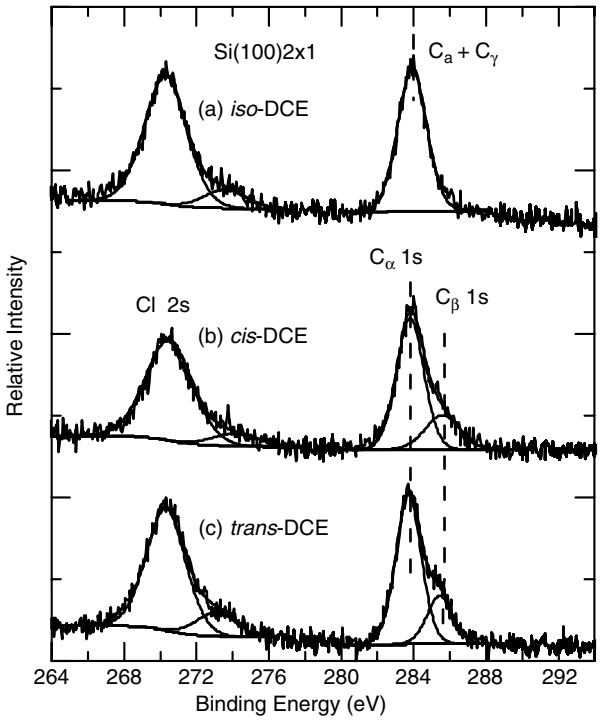

Fig. 1. C 1s and Cl 2s XPS spectra of 50 L (a) *iso*-, (b) *cis*- and (c) *trans*-dichloroethylene (DCE) exposed to Si(100)2 × 1 at room temperature.

energies of Cl 2s for Si–Cl and C–Cl obtained in our earlier [32] and present calculations (discussed below). A small shoulder with 7–8% of the total intensity is also observed at 273.9 eV. It should be noted no previous assignment for this feature is available in the literature. The large energy separation of this shoulder from the main Cl 2s peak (3.6 eV) could in theory be explained by the presence of Cl with a higher oxidation state (e.g., ClO_x), which is unlikely on the 2 × 1 surface. We can rule out the presence of ClO_x due to the lack of any corresponding O 1s signal in our XPS spectrum. Furthermore, the intensity and location of the Cl 2s shoulder is concomitantly increased or shifted with the main Cl 2s peak at 270.3 eV. We therefore assign this shoulder to a Cl 2s shake-up (many-body) process. In the C 1s region, the spectral envelopes of *cis*-DCE and *trans*-DCE are found to be similar to each other, but discernibly different from that of *iso*-DCE. In particular, the C 1s features at 283.9 eV and 285.6 eV for *cis*- and *trans*-DCE could be attributed to the ($=C_{\alpha}\!\!<^{H}_{Si}$) and ($=C_{\beta}\!\!<^{Cl}_{H}$) components, respectively, in good accord with our earlier work [32] and the spectra reported by Fink et al. [34].[1] The presence of the C_α (ipso C) component indicates dechlorination and, together with the presence of the C_β (non-ipso C) component, suggests the formation of mono-σ bonded 2-chlorovinyl adspecies. However, the intensity ratios of the C_α to C_β component are found to

[1] The subscripts for C are used to identify the C atoms in different local chemical environments, i.e. with different atoms attached. Similar notation has been used in our recent work [32].

be 2.8 and 3.1 for *cis*-DCE (Fig. 1b) [35] and *trans*-DCE (Fig. 1c), respectively, which shows that there are extra C_α components present, likely due to the formation of di-σ bonded vinylene adstructure involving double dechlorination. The approximately 3:1 intensity ratio of the C_α to C_β component further indicates equal surface concentrations between the vinylene and 2-chlorovinyl adstructures. In contrast, only one C 1s feature is found for *iso*-DCE (Fig. 1a), which shows that the local C chemical environments in the corresponding adstructures are similar. In the case of single dechlorination, we would expect the presence of two close-lying C 1s features corresponding to the $(=C_b\langle^{Cl}_{Si})$ component at 285.2 eV [32] and the $(=C_\eta\langle^{H}_{H})$ component at 284.8 eV [36] in the resulting 1-chlorovinyl adstructure. On the other hand, both the $(=C_a\langle^{Si}_{Si})$ and $(=C_\gamma\langle^{H}_{H})$ components in the vinylidene adstructure resulting from double dechlorination are expected to have similar C chemical environments to each other, because of the similar electronegativities of the Si (1.8, in the Pauling scale [37]) and H atoms (2.1). It should be noted that the local chemical environments of the C atoms in the $=C_\eta\langle^{H}_{H}$ and $=C_\gamma\langle^{H}_{H}$ components are different because of the different corresponding attaching C atoms: C_b and C_a, respectively. The presence of a single C 1s feature at 284.0 eV (and not at ~285 eV) therefore indicates the formation of vinylidene (instead of the 1-chorovinyl adspecies) as the predominant adstructure of *iso*-DCE. The C 1s energy location is also consistent with similar vinylidene feature observed in our recent work [32].

In order to elucidate the adsorption geometries for *cis*-, *trans*-, and *iso*-DCE, ab initio density functional calculations have been performed by using the Gaussian 03 program [38], with hybrid functionals consisting of Becke's three-parameter non-local exchange functional and the correlation functional of Lee–Yang–Parr (the so-called B3LYP method) [39]. The standard 6-31G(d) basis set has been used unless stated otherwise. A $Si_{15}H_{16}$ cluster was employed to approximate part of the Si(1 0 0)2 × 1 surface with two Si dimers. It should be noted that larger basis sets including 6-311G(d), 6-31++G(d) and 6-311++G(3df,3pd) have also been used. Although these basis sets are found to produce generally lower total energies as expected, they do not change the general geometries of the adstructures and the ordering of the stabilities of the adstructures. The use of larger basis sets therefore do not change the general conclusions inferred from the smaller basis sets. Two DCE molecules were used in order to study any adsorbate–adsorbate interactions and their subsequent effects on the adsorption process. Only the final geometrically optimized structures in these single-point energy calculations were considered in the present calculation. Based on our XPS spectra for the three DCE isomers on Si(1 0 0)2 × 1, we could infer four possible adstructures resulting from single and double dechlorination. Fig. 2a and b shows two 2-chlorovinyl adstructures (along with the dissociated Cl atoms) with similar adsorption energies ΔE and similar local C chemical environments for the $(=C_\alpha\langle^{H}_{Si})$ and $(=C_\beta\langle^{Cl}_{H})$ components. In particular, the 2-chlorovinyl conformer adstructure with the H atoms in the *cis* configuration ($\Delta E = -66.7$ kcal/mol, Fig. 2a) is slightly less stable than that with H atoms in the *trans* configuration ($\Delta E = -68.7$ kcal/mol, Fig. 2b). The origin of these two 2-chlorovinyl conformer adstructures could be due to the respective initial adsorption of *cis*- and *trans*-DCE, assuming that they both retain the original geometrical configurations upon dissociation. The small energy difference (2 kcal/mol) between the two conformer adstructures indicates that no thermodynamical preference for either adstructure, which is also consistent with the small energy difference found for *cis*- and *trans*-2-butenes (4 kcal/mol) as inferred by Kiskinova and Yates from their TPD data [28]. Furthermore, the two 2-chlorovinyl adstructures are expected to exhibit identical XPS spectra given their structural similarities. It is therefore impossible to rule out one or the other adstructure based on the XPS data alone.

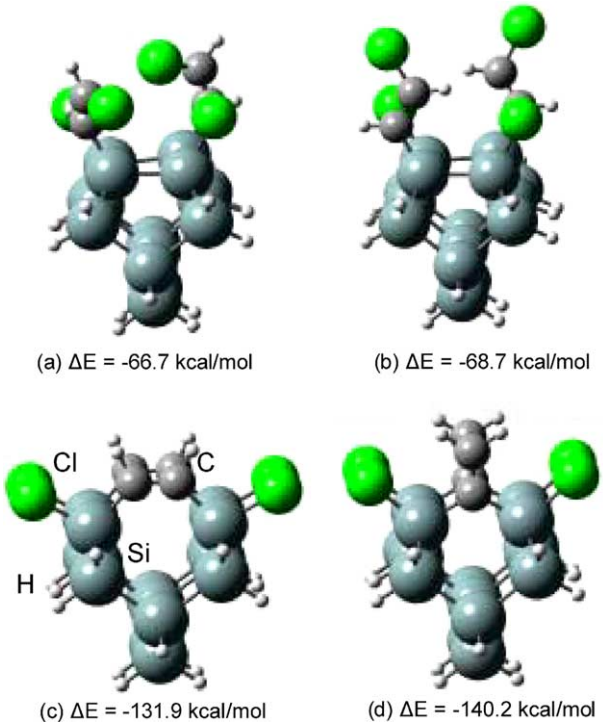

Fig. 2. Equilibrium geometries of four plausible adstructures for the three dichloroethylene (DCE) isomers on a model 2 × 1 surface of a $Si_{15}H_{16}$ cluster. The structures and their corresponding adsorption energies ΔE are obtained by density functional calculations at the B3LYP/6-31G(d) level. The two 2-chlorovinyl conformer adstructures (a, b) arise from single-dechlorination of *cis*- and *trans*-DCE, respectively, while vinylene (c) and vinylidene (d) come from double-dechlorination of *cis*- and *trans*-DCE and of *iso*-DCE, respectively.

Fig. 2c and d shows respectively the vinylene (with $\Delta E = -131.9$ kcal/mol) and vinylidene adstructures ($\Delta E = -140.2$ kcal/mol), both of which are considerably more stable than the 2-chlorovinyl adstructures (Fig. 2a and b). Given the molecular geometries for free *cis*-, *trans*- and *iso*-DCE, the vinylene adstructure (Fig. 2c) could result from double dechlorination of *cis*- and *trans*-DCE, while

vinylidene (Fig. 2d) could originate from double dechlorination of *iso*-DCE. Evidently, the vinylidene adstructure is found to be more stable than vinylene on the $Si_{15}H_{16}$ cluster by 8.3 kcal/mol [at the B3LYP/6-31G(d) level]. Furthermore, different local C environments are found in these adstructures, with C_α in ($=C_\alpha\langle^{H}_{Si}$) for vinylene (Fig. 2c), and C_γ in ($=C_\gamma\langle^{H}_{H}$) and C_a in ($=C_a\langle^{Si}_{Si}$) for vinylidene (Fig. 2d). Because of the similar electronegativities between Si (1.8) and H (2.1) [37], the C 1s binding energies for C_α (283.9 eV) [32], C_γ (284.0–284.8 eV) [36] and C_a (283.9 eV) [32] reported in the literature cannot be resolved with our present twin-anode XPS setup. The vinylene and vinylidene adstructures therefore could both give rise to an unresolved single C 1s feature near 283.9 eV, as shown in Fig. 1.

For ethylene on Si(1 0 0)2 × 1 [21] (and vinyl bromide on Si(1 0 0)c4 × 2 [8]), two possible adsorption mechanisms involving a tri-atom π-complex and a diradical intermediates have been proposed. Like ethylene, chlorinated ethylenes, such as *cis*- and *trans*-DCE, are believed to interact with the Si surface through the C atoms in the initial adsorption. We therefore expect that the formation of different final products, despite similar intermediates, is due to the presence of the Cl ligands. Fig. 3 shows the schematic diagrams of the possible adsorption mechanisms for *cis*- and *trans*-DCE and *iso*-DCE. For *cis*-DCE (Fig. 3a) and *trans*-DCE (Fig. 3b), interactions of the C 2p π orbitals with the upper Si dimer atom lead to the formation of the tri-atom π-complex intermediate (Structures 1 and 5). In ethylene, cycloaddition reaction is evidently preferred following the formation of the π-complex intermediate, likely because of the weaker bond strength of Si–H (71 kcal/mol) than C–H (81 kcal/mol) [27]. The slightly stronger bond strength of Si–Cl (109 kcal/mol) than C–Cl (95 kcal/mol) [27] therefore makes single dechlorination more plausible in the case of *cis*- and *trans*-DCE, producing the mono-σ bonded 2-chlorovinyl adspecies (Structures 2 and 6) and a dissociated Cl atom as the final surface products. The more electronegative Cl atom in the C–Cl bond is also compatible with the electropositive lower Si dimer atom,

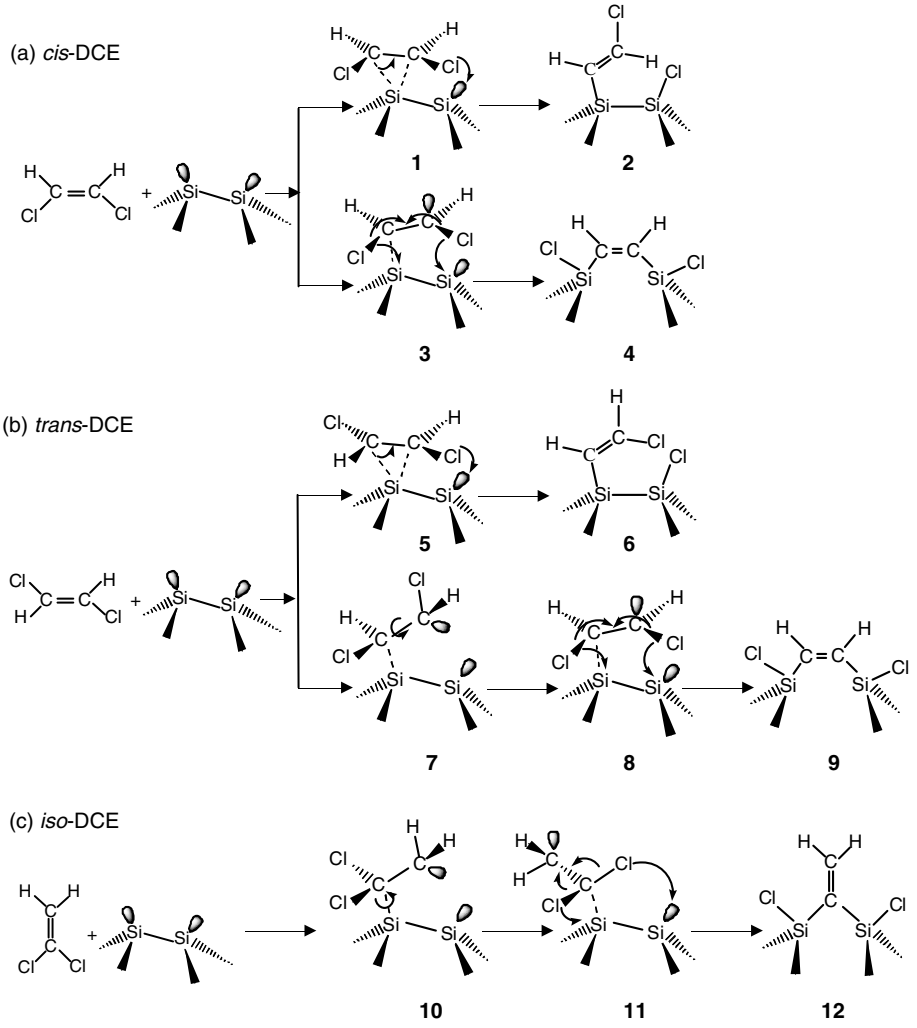

Fig. 3. Adsorption mechanisms involving the tri-atom π-complex and diradical intermediates for (a) *cis*-dichloroethylene (DCE) and (b) *trans*-DCE, and that involving the diradical intermediate for (c) *iso*-DCE.

thereby driving the dechlorination process. Furthermore, dechlorination of the tri-atom π-complex intermediate, with the C=C bond remaining intact during the process, preserves the original *cis* and *trans* conformations of the H atoms in the respective 2-chlorovinyl conformers (Structures 2 and 6). On the other hand, breaking the C=C π-bond in *cis*-DCE (Fig. 3a) or *trans*-DCE (Fig. 3b) leads to the formation of a diradical intermediate (Structures 3 and 8). Upon adsorption, the diradical intermediate undergoes double dechlorination (Structures 3 and 8), thereby reforming the C=C bond and producing the vinylene adstructure (Structures 4 and 9). It should be noted that the breaking of the C=C bond and the subsequent free rotation around the resulting C–C bond causes the loss of the original *cis* and *trans* geometrical registries, as illustrated by the transition from Structure 7 to Structure 8 in Fig. 3b. This pathway therefore produces the same adspecies, vinylene, for both *cis*- and *trans*-DCE. The present diradical pathway is consistent with those proposed for *cis*- and *trans*-DCE on Pt(1 1 1) by Grassian and Pimentel [30], who observed the saturation and subsequent reformation of the C=C bond by dechlorination upon annealing from 110 K to 270 K. The formation of 2-chlorovinyl and vinylene adspecies and their nearly equal surface concentrations as observed from our XPS spectra (Fig. 1) support no particular preference for either the tri-atom π-complex or diradical intermediate pathway. However, given the large differences in the thermodynamical stabilities of the 2-chlorovinyl ($\Delta E = -66.7$ to -68.7 kcal/mol) and vinylene adstructures ($\Delta E = -131.9$ kcal/mol), the lack of preference therefore indicates that the formation of the tri-atom π-complex or diradical intermediates is likely controlled by kinetic factors.

In the case of *iso*-DCE, the presence of the single C 1s feature at 284.0 eV (Fig. 1c) indicates the formation of vinylidene by double dechlorination through the diradical intermediate. As shown in Fig. 3c, the free rotation around the Si–C bond of the adsorbed diradical intermediate (Structure 10) facilitates both Cl atoms (attached to the ipso C) to be in close proximity (Structure 11) to form, upon breakage of the C–Cl bonds, the more stable Si–Cl bonds. The resulting vinylidene in effect bridges the two Si dimer atoms through a single ipso C (Structure 12), giving rise to the most stable adstructure shown in Fig. 2d. Although both geometrical isomers (*cis*- and *trans*-DCE) and *iso*-DCE all react on Si(1 0 0)2 × 1 through the diradical intermediate pathway, the different locations of the Cl atoms in the isomer structure lead to different dechlorination products (vinylene and vinylidene, respectively). The observed difference in the end-products therefore demonstrates a direct structural isomer effect. The differences in the isomer structures cause different atomic charge distributions on the C atoms, which in turn lead to different pathways and end-products. In the case of *iso*-DCE, the attachment of both Cl atoms produces a strong electron-withdrawing effect on the C atom (with an APT atomic charge of +0.76 a.u. as estimated by our density functional calculation), in marked contrast to the attachment of both H atoms that produces a negative APT charge of −0.30 a.u. on the C atom. For *cis*- and *trans*-DCE, the respective C atoms (each with a Cl and a H atom attached) are less electrophilic, with an APT charge of +0.20 a.u and +0.25 a.u. respectively. Given that the upper dimer Si atom is generally recognized to be more electronegative than the lower dimer atom in the asymmetric Si dimer (or buckled dimer) model [23], only the electropositive C atom in the ($=C\begin{smallmatrix}\diagup Cl\\ \diagdown Cl\end{smallmatrix}$) component could therefore interact with the upper dimer atom, and only the diradical pathway is therefore plausible for *iso*-DCE (Fig. 3c). On the other hand, the equally positively charged C atoms in *cis*-DCE (Fig. 3a) and *trans*-DCE (Fig. 3b) enable the formation of the tri-atom π-complex intermediate, in addition to the diradical intermediate.

For *cis*- and *trans*-butene on Si(1 0 0)2 × 1, Lopinski et al. reported that adsorption occurs predominantly through the tri-atom π-complex intermediate pathway, with only ~2% involving the diradical intermediate pathway [40]. In the present case, replacement of the methyl groups with the more electron-withdrawing Cl atoms is expected to weaken the π-bond of the C=C backbone, thereby strongly favouring the diradical intermediate pathway. In support of this hypothesis, our calculations also show that the corresponding APT charges for the C atoms in the C=C bond of *cis*-butene (+0.0045 a.u.) and *trans*-butene (+0.089 a.u.) are less positive than those found for *cis*-DCE (+0.20 a.u.) and *trans*-DCE (+0.25 a.u.), each with a more electron-withdrawing Cl ligand (per C atom). The correspondingly lower π-electron densities in the C=C bonds in *cis*- and *trans*-DCE could therefore account for the considerably larger fraction (50%) of adsorption involving the diradical intermediate. Furthermore, in the case of *iso*-DCE the addition of a second Cl ligand to the same C atom results in an even larger electrophilic center, which exclusively favours the diradical intermediate pathway.

3.2. Thermal evolution

Fig. 4 compares the temperature-dependent XPS spectra of 50 L *trans*-DCE with those of *iso*-DCE on Si(1 0 0)2 × 1. The temperature-dependent XPS spectra of *cis*-DCE have been reported earlier by us [32] and are found to be very similar to those of *trans*-DCE. The corresponding fitted intensities of the respective C 1s and Cl 2s features, with respect to that of the Si 2p feature at 99.3 eV, are also shown as a function of the flash-annealing temperature in Fig. 4. Like *cis*-DCE [32], the C_α 1s feature at 283.9 eV and the C_β 1s feature at 285.6 eV of *trans*-DCE appear to be stable to 435 K (Fig. 4a). Annealing the sample to 620 K evidently converts the C_β component to C_α, indicating further dechlorination of the 2-chlorovinyl adspecies to the vinylene adstructure. Upon further annealing to 800 K, the C_β component has essentially disappeared while the C_α component has begun to reduce in intensity and to shift to a

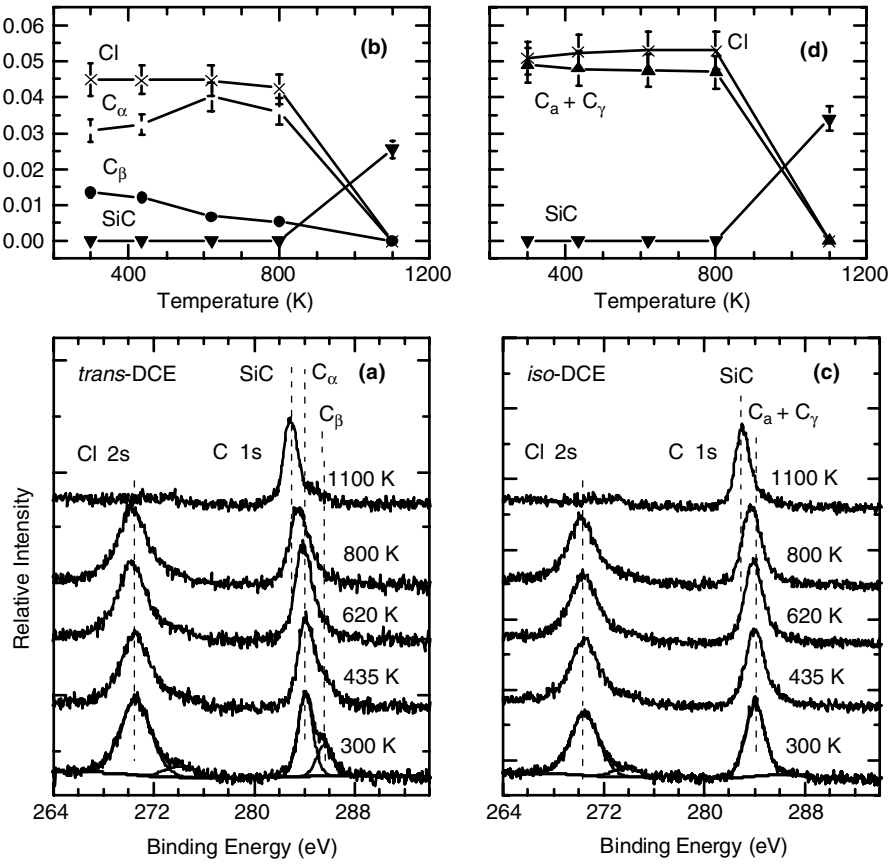

Fig. 4. Temperature-dependent C 1s and Cl 2s XPS spectra of 50 L (a) *trans*-dichloroethylene (DCE) and (c) *iso*-DCE. The relative intensities (I) with respect to Si 2p feature for the C 1s features at 283.9 eV (C_α, ■), 285.6 eV (C_β, ●), 284.0 eV ($C_a + C_\gamma$, ▲), and 283.0 eV (SiC, ▼) and for the Cl 2s features at 270.3 eV (×) are shown in (b) and (d).

lower binding energy, depicting total destruction of the 2-chlorovinyl adspecies and decomposition of the vinylene adspecies. The reduction in the total C 1s relative intensity from 620 K to 800 K indicates desorption of the C-containing adspecies (Fig. 4b). Above 800 K, the C-containing adspecies has further evolved to SiC, with a characteristic C 1s binding energy of 283.0 eV, and/or diffused into the bulk, as clearly shown in the spectrum obtained at 1100 K. For the Cl 2s envelope, the intensity remains nearly constant below 800 K (Fig. 4b), which shows that the dissociated Cl atoms resulting from dechlorination of various adspecies above 435 K remain largely on the surface. Further annealing the sample to 1100 K totally diminishes the Cl 2s intensity, indicating the removal of the dissociated Cl atoms from the surface at 800–1100 K.

For *iso*-DCE (Fig. 4c and d), the single C 1s feature at 284.0 eV, previously attributed to the ($=C_a\swarrow^{Si}_{Si}$) and ($=C_\gamma\swarrow^{H}_{H}$) components of vinylidene (Fig. 2d), is found to remain largely unchanged in its energy position and intensity upon annealing to 620 K. In accord with our calculations, the vinylidene adstructure (Fig. 2d) is therefore more thermally stable than the 2-chlorovinyl adspecies (Fig. 2a and b) resulting from the *cis*-DCE and *trans*-DCE adsorption, which dechlorinates above 435 K (Fig. 4a). Furthermore, the observed shift to a lower binding energy and discernible weakening of the C 1s feature over the temperature range 620–800 K indicates decomposition and/or desorption of the vinylidene adspecies. Upon further annealing the sample to 1100 K, the C 1s peak is found to evolve into the SiC feature at 283.0 eV, which confirms total destruction of the remaining adspecies at this high temperature. The thermal evolution of the Cl 2s feature for *iso*-DCE (Fig. 4d) follows that observed for *cis*-DCE [32] and *trans*-DCE (Fig. 4b), in general accord with the aforementioned thermal evolution of dissociated Cl atoms.

In order to investigate the desorption products during the thermal evolution process, TPD profiles of selected ions for saturation exposures (50 L) of *cis*- and *trans*-DCE as well as *iso*-DCE are obtained and shown in Fig. 5. Following our earlier work on *cis*-DCE [32,35], we focus on the thermal evolution of similar ions, particularly the parent ions of HCl, C_2H_2 and H_2 with *m*/*z* 36, 26 and 2, respectively. Other fragments including those with *m*/*z* 96 ($C_2H_2Cl_2^+$ or the parent ion), 94 ($C_2Cl_2^+$) and 61 ($C_2H_2Cl^+$) have also been monitored but exhibited no discernible desorption features. The absence of the parent ions of DCE is therefore consistent with dechlorination of DCE upon adsorption, as inferred from our XPS data (Fig. 1). It should be noted the three sets of TPD profiles for the dif-

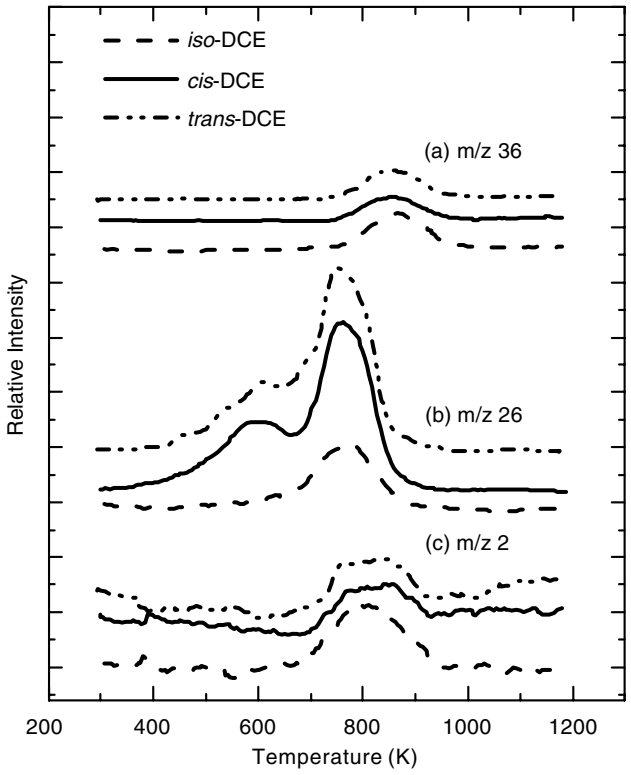

Fig. 5. Temperature programmed desorption profiles of (a) m/z 36 (HCl^+), (b) m/z 26 ($C_2H_2^+$) and (c) m/z 2 (H_2^+) for 50 L *iso*-, *cis*- and *trans*-dichloroethylene (DCE) exposed to Si(1 0 0)2 × 1 at room temperature. The profiles for individual DCE isomers have been offset for clarity.

ferent isomers have been normalized to one another on the averaged background of m/z 2 over the temperature range 300-600 K. Like *cis*-DCE on Si(1 0 0)2 × 1 [32,35], the two m/z 26 desorption features for *trans*-DCE (Fig. 5b) could be similarly attributed to C_2H_2 desorption, respectively, from mono-σ bonded 2-chlorovinyl adspecies upon Cl elimination near 590 K and from di-σ bonded vinylene adspecies upon breakage of two Si–C bonds near 750 K. In contrast, only the m/z 26 desorption peak at 780 K corresponding to C_2H_2 desorption from the di-σ bonded vinylidene adspecies is observed for *iso*-DCE. The absence of the m/z 26 desorption feature at a lower temperature for *iso*-DCE supports our earlier observation of total dechlorination upon RT adsorption of *iso*-DCE. Furthermore, the total intensities of the m/z 26 desorption profiles for *cis*-DCE and *trans*-DCE are found to be essentially the same, while that for *iso*-DCE is considerably smaller (25%). Evidently, thermal evolution of the corresponding vinylidene adspecies to C_2H_2 desorbate is less probable, likely because additional H rearrangement is required. In addition, all three isomers exhibit a m/z 2 desorption feature at 800 K, characteristic of recombinative desorption of H_2 from Si monohydrides (Fig. 5c) [10]. The formation of monohydrides corresponds to dissociation of vinylene adspecies in the case of *cis*- and *trans*-DCE and of vinylidene adspecies for *iso*-DCE on Si(1 0 0)2 × 1. It should be noted that 2-chlorovinyl adspecies (for *cis*- and *trans*-DCE adsorption) has been found to undergo dechlorination to vinylene at 590 K before H abstraction could take place [32]. Like the m/z 26 desorption features, the intensity of the m/z 2 feature (Fig. 5c) for *cis*-DCE is also found to be nearly identical to that for *trans*-DCE, which confirms that the remaining adspecies after C_2H_2 evolution undergo similar H abstraction for both *cis*-DCE and *trans*-DCE. The considerably stronger m/z 2 desorption feature for *iso*-DCE than *cis*- and *trans*-DCE (by over 70%) is consistent with H abstraction of a larger amount of vinylidene adspecies that do not undergo C_2H_2 evolution (Fig. 5b). Finally, a single TPD feature of m/z 36 extending over 780–930 K with desorption maximum at 850 K has been observed for all three isomers (Fig. 5a). This feature corresponds to recombinative desorption of HCl from dissociated Cl atoms (as a result of dechlorination) and H atoms from Si monohydrides. Furthermore, the m/z 36 desorption intensities for all three isomers are found to be similar, indicating that all three isomers produce similar amounts of Cl atoms upon total dechlorination and that HCl evolution is evidently the only removal channel of the dissociated Cl atoms.

4. Summary

Room-temperature chemisorption and thermal evolution of *cis*-DCE and *trans*-DCE as well as their structural isomer, *iso*-DCE, on Si(1 0 0)2 × 1 have been investigated by using XPS and TPD techniques. The equilibrium geometries of plausible adstructures are obtained by density functional calculations at the B3LYP/6-31G(d) level. Evidently, all three isomers are found to undergo dechlorination upon RT adsorption on the 2 × 1 surface. The dissociated Cl atoms are thermally stable on the 2 × 1 surface and desorb as HCl only near 850 K. The nature of the RT adsorption and the thermal evolution of adstructures for *cis*- and *trans*-DCE on the 2 × 1 surface are found to be remarkably similar to each other. In particular, both isomers give rise to 2-chlorovinyl and vinylene adstructures at RT through single and double dechlorination, respectively. The 2-chlorovinyl adspecies is found to undergo further dechlorination at 590 K to vinylene, which is stable to 750 K. Both thermal evolution processes also give rise to acetylene as the desorption product. On the other hand, *iso*-DCE adsorbs on Si(1 0 0)2 × 1 through total dechlorination at RT and forms a di-σ bonded vinylidene adspecies. Like vinylene, the vinylidene adstructure appears to be quite stable and desorbs as acetylene near 780 K. Above 800 K, formation of SiC is observed for all three isomers.

Two adsorption mechanisms involving a tri-atom π-complex and a diradical intermediates have been proposed for the DCE isomers. In particular, the tri-atom π-complex intermediate gives rise to the mono-σ bonded 2-chlorovinyl adspecies, while the diradical intermediate results in the di-σ bonded vinylene adspecies observed for *cis*- and *trans*-DCE. The formation of the diradical intermediate requires the breaking of the C=C bond, and the free rotation

around the resulting C–C single bond causes the loss of *cis* and *trans* geometrical registries, which accounts for non-conformational specificity upon the formation of vinylene. The equally positively charged C atoms in *cis*- and *trans*-DCE enable the formation of both the tri-atomic π-complex and diradical intermediates. Our XPS data show that both 2-chlorovinyl and vinylene surface products, and their corresponding pathways, are equally probable. However, our density functional calculations indicate that vinylene (with $\Delta E = -131.1$ kcal/mol) is more thermodynamically stable than the 2-chlorovinyl adstructure (with $\Delta E = -66.7$–68.7 kcal/mol), which therefore suggests that kinetic effects play a more important role in the adsorption process of *cis*- and *trans*-DCE. On the other hand, the attachment of both Cl atoms on a single C atom in *iso*-DCE produces a strong electron-withdrawing effect, which favours the predominant formation of the diradical intermediate. The differences in the isomer structures between *cis*- and *trans*-DCE and their structural isomer, *iso*-DCE, (with their correspondingly different atomic charge distributions on the C atoms) therefore produce a directly observable structural isomer effect, which is responsible for the different pathways and the observed end-products. It is of interest to note that in the case of ethylene or acetylene [24,25] the proposed tri-atom π-complex and diradical pathways both lead to a single cycloaddition surface product because of the absence of Cl atoms and the corresponding dechlorination process as found in the present DCE cases.

The combination of the XPS and TPD data has provided a clear picture of the RT adsorption of the three DCE isomers on Si(1 0 0)2 × 1 and the thermal evolution of their respective adstructures. Upon RT adsorption of the three isomers, the Si surface atoms are effectively terminated by the dissociated Cl atoms, which could provide a 1 × 1 surface template. For *cis*- and *trans*-DCE, the mixture of 2-chlorovinyl and vinylene adstructures could be used as building blocks for consolidating a 2 × 1 array of vinylene bridging between the Si dimer atoms by annealing to 590 K, as shown in Fig. 6a. On the other hand, a similar 2 × 1 array of vinylidene adstructure (Fig. 6b) could be generated by exposing *iso*-DCE to the 2 × 1 surface at RT. Like the vinylene array, this vinylidene template evidently could remain quite stable, up to a temperature near 780 K. It is of interest to note that while both vinylene and vinylidene occupy the same relative template positions, the C=C bond in vinylene is surface parallel to the dimer row, in contrast to that in vinylidene oriented perpendicularly to the surface. It may therefore be possible to produce a two-dimensional array of C=C bonds selectively oriented by appropriate choice of the DCE isomers. These arrays may offer useful interfaces for further organic functionalization of the Si surface.

Finally, it is of interest to compare the thermally driven surface chemistry of the three DCE isomers on Si(1 0 0)2 × 1 with that on Si(1 1 1)7 × 7 [31]. In particular, all three isomers are found to undergo dechlorination upon

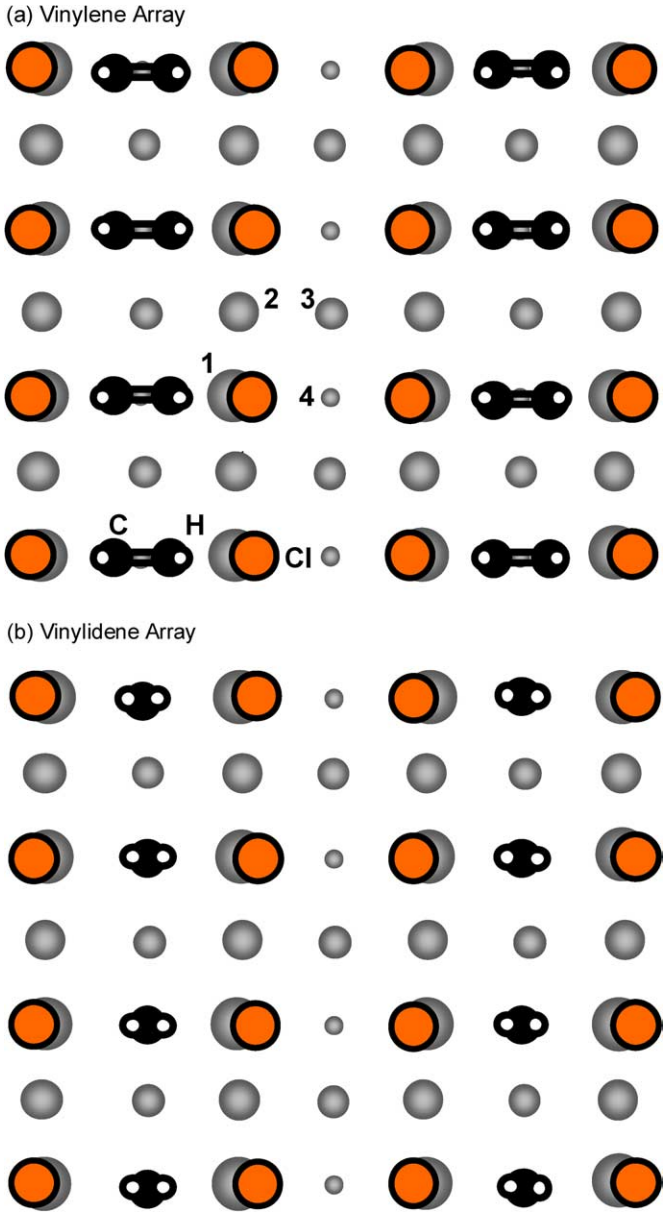

Fig. 6. Schematic diagrams of ordered arrays of Cl atoms at the 1 × 1 sites with overlapping arrays of (a) vinylene and (b) vinylidene at the 2 × 1 sites. Si atoms in the top (surface, layer 1) to bottom layers (layer 4) are represented by grey circles of decreasing diameters, while the Cl, C and H atoms are shown as open shaded circles, solid black circles and open white circles, respectively.

adsorption on both Si(1 0 0)2 × 1 and Si(1 1 1)7 × 7 surfaces at RT. Furthermore, m/z 26 ($C_2H_2^+$), m/z 36 (HCl^+) and m/z 2 (H_2^+) are also found to be the common desorbates at similar desorption temperature ranges in the thermal evolution of all three isomers on both surfaces. For the 7 × 7 surface, additional etching product $SiCl_2$ at 800–950 K is observed for the three isomers, which suggests that there are more H atoms remaining on the 2 × 1 surface. For *cis*-DCE and *trans*-DCE, mono-σ bonded 2-chlorovinyl adspecies appears to be the common RT adspecies on both surfaces, while the di-σ-bonded vinylene adspecies, observed as the other equally probable RT adspecies on the

2×1 surface, is found only upon annealing above 450 K on the 7×7 surface. The lack of double dechlorination at RT on the 7×7 surface could be due to incompatibility of vinylene with the local geometries of the available Si adsorption sites. The 2×1 surface therefore readily facilitates dechlorination reactions, in accord with the generally higher reactivity of the Si(1 0 0)2×1 surface than the Si(1 1 1)7×7 surface. There is also no stereoisomeric effect for the 2×1 surface, in contrast to the 7×7 surface which exhibits stronger dechlorination reactivity towards *trans*-DCE than *cis*-DCE. The formation of vinylidene only from *iso*-DCE does nicely illustrate a structural isomer effect on both Si(1 0 0)2×1 and Si(1 1 1)7×7 surfaces. However, the vinylidene adspecies appears to be stable to a relatively high temperature (>700 K) on the 2×1 surface, unlike its continued evolution to vinylene above 450 K on the 7×7 surface. This difference is likely due to the geometrical incompatibility of the Si(1 1 1)7×7 surface with vinylidene. The complexity and multitude of the available bonding sites on the Si(1 1 1)7×7 surface therefore make the 7×7 surface a less favourable choice as a substrate for the fabrication of ordered C=C containing molecular arrays.

Acknowledgment

This work was supported by the Natural Sciences and Engineering Research Council of Canada.

References

[1] R.A. Wolkow, Ann. Rev. Phys. Chem. 50 (1999) 413.
[2] C.C. Cheng, R.M. Wallace, P.A. Taylor, W.J. Choyke, J.T. Yates Jr., J. Appl. Phys. 67 (1990) 3693.
[3] M. Nagao, Y. Yamashita, S. Machida, K. Hamaguchi, F. Yasui, K. Mukai, J. Yoshinbu, Surf. Sci. 513 (2002) 413.
[4] M.P. Schwartz, M.D. Ellison, S.K. Coulter, J.S. Hovis, R.J. Hamers, J. Am. Chem. Soc. 122 (2000) 8529.
[5] M.J. Kong, A.V. Teplyakov, J.G. Lyubovitsky, S.F. Bent, Surf. Sci. 411 (1998) 286.
[6] N.P. Guisinger, R. Basu, A.S. Baluch, M.C. Hersam, Ann. NY Acad. Sci. 1006 (2003) 227.
[7] Z.H. He, X. Yang, X.J. Zhou, K.T. Leung, Surf. Sci. 547 (2003) L840.
[8] M. Nagao, K. Mukai, Y. Yamashita, J. Yoshinobu, J. Phys. Chem. B 108 (2004) 5703.
[9] W. Widdra, C. Huang, G.A.D. Briggs, W.H. Weinberg, J. Electron, Spect. Relat. Phenom. 64 (1993) 129.
[10] P.A Taylor, R.M. Wallace, C.C. Cheng, W.H. Weinberg, M.J. Dresser, W.J. Choyke, J.T. Yates Jr., J. Am. Chem. Soc. 114 (1992) 6754.
[11] Q. Li, Z.H. He, X.J. Zhou, X. Yang, K.T. Leung, Surf. Sci. 560 (2004) 191.
[12] Q. Li, K.T. Leung, Surf. Sci. 479 (2001) 69.
[13] Q. Li, K.T. Leung, Surf. Sci. 541 (2003) 111.
[14] X.J. Zhou, Q. Li, Z.H. He, X. Yang, K.T. Leung, Surf. Sci. 543 (2003) L668.
[15] L. Fang, J. Liu, S. Coulter, X.P. Cao, M.P. Schwartz, C. Hacker, R.J. Hamers, Surf. Sci. 514 (2002) 362.
[16] G.P. Lopinski, D.J. Moffatt, R.A. Wolkow, Chem. Phys. Lett. 282 (1998) 305.
[17] Y. Cao, X.M. Wei, W.S. Chin, Y.H. Lai, J.F. Deng, S.L. Bernasek, G.Q. Xu, J. Phys. Chem. B 103 (1999) 5698.
[18] C.S. Carmer, B. Weiner, M. Frenklach, J. Chem. Phys. 99 (1993) 1356.
[19] R. Miotto, A.C. Ferraz, G.P. Srivastava, Surf. Sci. 507–510 (2002) 12.
[20] W. Widdra, A. Fink, S. Gokhale, P. Trischberger, D. Menzel, Phys. Rev. Lett. 80 (1998) 4269.
[21] X. Lu, M.P. Zhu, X.L. Wang, J. Phys. Chem. B 108 (2004) 7359.
[22] M.A. Filler, S.F. Bent, Prog. Surf. Sci. 73 (2003) 1.
[23] Q. Liu, R. Hoffmann, J. Am. Chem. Soc. 117 (1995) 4082.
[24] H. Liu, R.J. Hamers, J. Am. Chem. Soc. 119 (1997) 7593.
[25] X. Lu, J. Am. Chem. Soc. 125 (2003) 6384.
[26] M.X. Yang, P.W. Kash, D.-H. Sun, G.W. Flynn, B.E. Bent, M.T. Holbrook, S.R. Bare, J.L. Gland, D.A. Fischer, Surf. Sci. 380 (1997) 151.
[27] R.C. Weast (Ed.), CRC Handbook of Chemistry and Physics, 64th ed., CRC Press, Baton Raton, 1983.
[28] M. Kiskinova, J.T. Yates Jr., Surf. Sci. 325 (1995) 1.
[29] G.P. Lopinski, D.J. Moffatt, D.D.M. Wayner, R.A. Wolkow, J. Am. Chem. Soc. 122 (2000) 3548.
[30] V.H. Grassian, G.C. Pimentel, J. Chem. Phys. 88 (1988) 4478.
[31] Z.H. He, Q. Li, K.T. Leung, Surf. Sci., this issue, doi:10.1016/j.susc.2005.11.003.
[32] X.J. Zhou, K.T. Leung, J. Phys. Chem. B, submitted for publication.
[33] J.F. Moulder, W.F. Stickle, P.E. Sobol, K.D. Bomben, Handbook of X-ray Photoelectron Spectroscopy, Perkin-Elmer Corporation, Minnesota, USA, 1992.
[34] A. Fink, W. Widdra, W. Wurth, C. Keller, M. Stichler, A. Achleitner, G. Comelli, S. Lizzit, A. Baraldi, D. Menzel, Phys. Rev. B 64 (2001) 045308.
[35] X.J. Zhou, K.T. Leung, Chem. Phys. Lett., submitted for publication.
[36] X. Cao, S.K. Coulter, M.D. Ellison, H. Liu, J. Liu, R.J. Hamers, J. Phys. Chem. B 105 (2001) 3759.
[37] L. Pauling, The Nature of Chemical Bond, Cornell University Press, Ithaca, 1960.
[38] Gaussian 03 Revision A.1, M.J. Frisch, G.W. Trucks, H.B. Schlegel, G.E. Scuseria, M.A. Robb, J.R. Cheeseman, J.A. Montgomery Jr., T. Vreven, K.N. Kudin, J.C. Burant, J.M. Millam, S.S. Iyengar, J. Tomasi, V. Barone, B. Mennucci, M. Cossi, G. Scalmani, N. Rega, G.A. Petersson, H. Nakatsuji, M. Hada, M. Ehara, K. Toyota, R.Fukuda, J. Hasegawa, M. Ishida, T. Nakajima, Y. Honda, O. Kitao, H. Nakai, M. Klene, X. Li, J.E. Knox, H.P. Hratchian, J.B. Cross, C. Adamo, J. Jaramillo, R. Gomperts, R.E. Stratmann, O. Yazyev, A.J. Austin, R. Cammi, C. Pomelli, J.W. Ochterski, P.Y. Ayala, K. Morokuma, G.A. Voth, P. Salvador, J.J. Dannenberg, V.G. Zakrzewski, S. Dapprich, A.D. Daniels, M.C. Strain, O. Farkas, D.K. Malick, A.D. Rabuck, K. Raghavachari, J.B. Foresman, J.V. Ortiz, Q. Cui, A.G. Baboul, S. Clifford, J. Cioslowski, B.B. Stefanov, G. Liu, A. Liashenko, P. Piskorz, I. Komaromi, R.L. Martin, D.J. Fox, T. Keith, M.A.Al-Laham, C.Y. Gonzalez, J.A. Pople, Gaussian, Inc., Pittsburgh PA, 2003.
[39] J.B. Foresman, Æ. Frisch, Exploring Chemistry with Electronic Structure Methods, second ed., Gaussian Inc., Pittsburgh, 1996, and references therein.
[40] G.P. Lopinski, D.J. Moffatt, D.D. Wayner, R.A. Wolkow, Nature 392 (1998) 909.